International Journal of Pharmaceutics 597 (2021) 120199

Contents lists available at ScienceDirect

International Journal of Pharmaceutics

journal homepage: www.elsevier.com/locate/ijpharm

Preparation, stabilisation, isolation and tableting of valsartan nanoparticles using a semi-continuous carrier particle mediated process

Ajay Kumar [a,b], Kiran A. Ramisetty [a,b], Simone Bordignon [a], Benjamin K. Hodnett [a,b], Peter Davern [a,b], Sarah Hudson [a,b,*]

[a] Synthesis and Solid State Pharmaceutical Centre, Department of Chemical Sciences, and The Bernal Institute, University of Limerick, Limerick V94 T9PX, Ireland
[b] SSPC the Science Foundation Ireland Research Centre for Pharmaceutics, University of Limerick, Limerick V94 T9PX, Ireland

ARTICLE INFO

Keywords:
Carrier particle mediated semi-continuous process
Reverse antisolvent precipitation
Drug nanoparticles
Robust process
Tableting
Dissolution rate

ABSTRACT

This work investigated the technical feasibility of preparing, stabilizing and isolating poorly water-soluble drug nanoparticles via a small-scale antisolvent precipitation process operating in semi-continuous mode. Specifically, a novel semi-continuous process was demonstrated for the carrier particle mediated production, stabilization and isolation of valsartan nanoparticles into a solid form using montmorillonite clay particles as the carrier. The semi-continuous process operated robustly for the full duration of the experiment (~16 min) and steady-state conditions were reached after ~5 min. Nanoparticles of valsartan (51 ± 1 nm) were successfully prepared, stabilized and isolated with the help of montmorillonite (MMT) or protamine functionalized montmorillonite (PA-MMT) into the dried form by this semi-continuous route. The dissolution profile of the isolated valsartan nanocomposite solids was similar to that of valsartan nanocomposite solids produced via the corresponding laboratory scale batch mode process, indicating that the product quality (principally the nanoscale particle size and solid-state form) is retained during the semi-continuous processing of the nanoparticles. Furthermore, tablets produced via direct compression of the isolated valsartan nanocomposite solids displayed a dissolution profile comparable with that of the powdered nanocomposite material. PXRD, DSC, SSNMR and dissolution studies indicate that the valsartan nanoparticles produced via this semi-continuous process were amorphous and exhibited shelf-life stability equivalent to > 10 months.

1. Introduction

Pharmaceutical crystallization is typically carried out in batch reactors using cooling, normal and reverse antisolvent addition, evaporation, pH adjustment or chemical reaction to generate supersaturated solutions that induce solute molecules to come together to nucleate and grow into crystals (Quon et al., 2012; Nagy and Braatz, 2012). However, in recent years, there has been increased industrial and academic interest in changing pharmaceutical processing from batch to more efficient continuous processes (Poechlauer et al., 2012; Mascia et al., 2013; Wong et al., 2012; Myerson et al., 2014; Tung, 2013; Jiang and Braatz, 2019). Continuous manufacturing provides several potential opportunities, such as better control of product quality, lower costs, greater reliability and safety, better sustainability and increased flexibility (Eder et al., 2010; Jiang et al., 2014; Zhang et al., 2012). Although batch operation is the more common and well-understood approach, there are still significant issues associated with it, such as batch to batch variability, difficulty in scaling up and producing homogeneous processing conditions, which can lead to substantial issues in downstream processes, subsequent formulation into medicines and *in vivo* performance (Quon et al., 2012; Zhang et al., 2012; Plumb, 2005; Chen et al., 2011). Continuous manufacturing has inherent advantages over batch with

Abbreviations: APIs, active pharmaceutical ingredients; MMT, montmorillonite K10; PA, protamine sulphate salt; PXRD, powder X-ray diffraction; DSC, differential scanning calorimetry; NCs, nanocomposites; NPs, nanoparticles; Val-MMT, valsartan montmorillonite; Val-PA-MMT, valsartan-protamine-montmorillonite; SSNMR, solid-state nuclear magnetic resonance; CPMAS, ^{13}C cross-polarization magic-angle spinning; CMC, carboxymethyl cellulose; TPPM, two-pulse phase modulation.

* Corresponding author at: SSPC, SFI Research Centre for Pharmaceuticals, Department of Chemical Sciences, and Bernal Institute, University of Limerick, Limerick V94 T9PX, Ireland.

E-mail addresses: Ajay.Kumar@ul.ie (A. Kumar), Kirankumar.Ramisetty@ul.ie (K.A. Ramisetty), simone.bordignon@unito.it (S. Bordignon), Kieran.Hodnett@ul.ie (B.K. Hodnett), Peter.Davern@ul.ie (P. Davern), Sarah.Hudson@ul.ie (S. Hudson).

https://doi.org/10.1016/j.ijpharm.2021.120199
Received 8 September 2020; Received in revised form 28 November 2020; Accepted 20 December 2020
Available online 21 January 2021

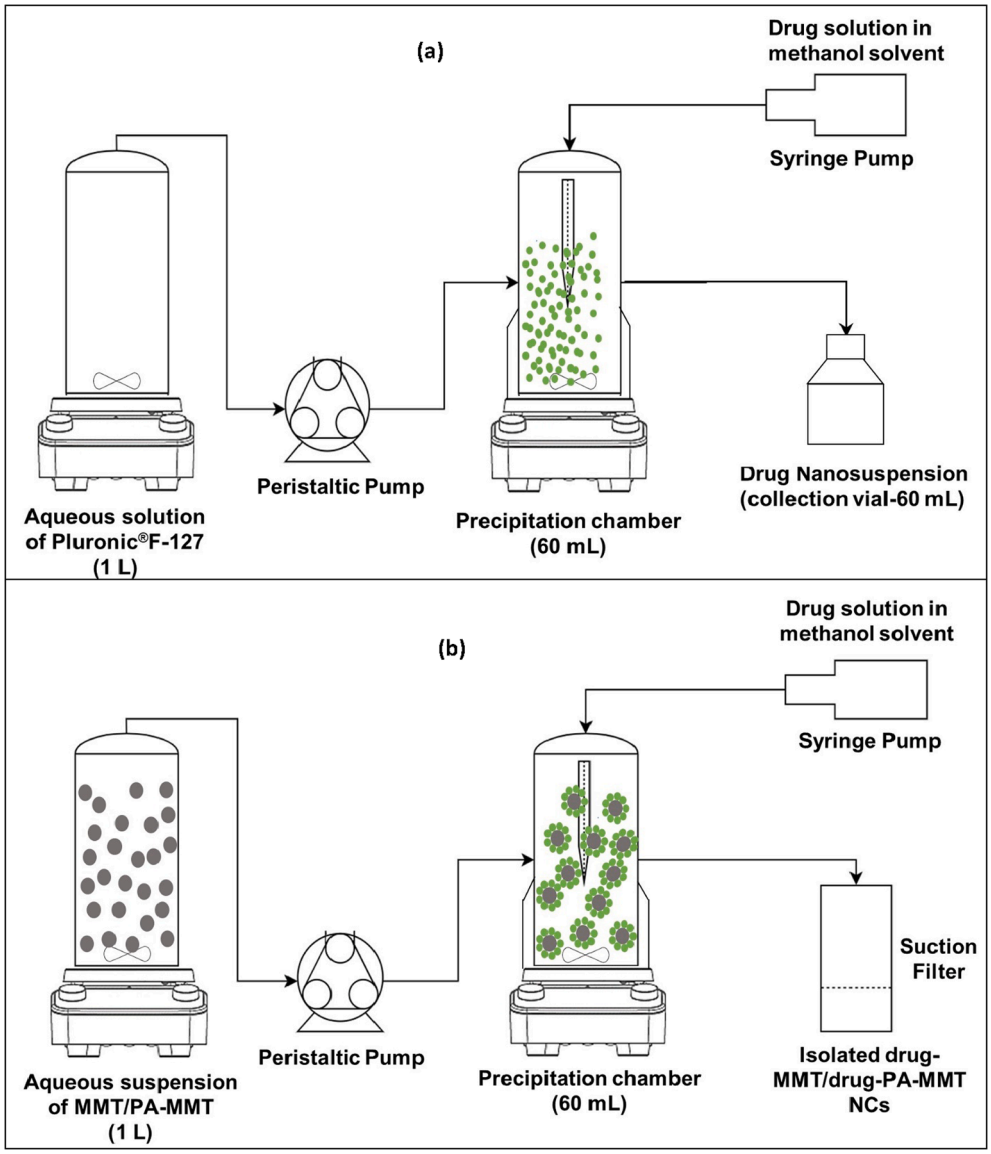

Fig. 1. A schematic illustration of (a) the semi-continuous preparation of valsartan nanosuspension stabilized by Pluronic® F-127 and (b) the semi-continuous preparation, stabilization by MMT/PA-MMT, and isolation of valsartan nanocomposites by filtration.

respect to process control. The steady-state is usually easier to control due to tighter equipment integration as well as a higher level of automation (Mascia et al., 2013; Lakerveld et al., 2015; Heider et al., 2014; Lakerveld et al., 2013; Hadiwinoto et al., 2019).

Drug nanoparticles at an industrial scale are mainly produced by "top-down" techniques such as milling and high-pressure homogenization, which basically break down large crystalline drug particles into nanoparticles (Keck and Muller, 2006; Dong et al., 2010). In contrast, "bottom-up" techniques, which are based on controlled precipitation/crystallization to form nanoparticles by building up particles from the molecular state, are rarely used at the industrial scale (Horn and Rieger, 2001; Rogers et al., 2004). One such bottom-up technique, liquid antisolvent precipitation, is a fast, simple and cost-efficient method of nanoparticle production. It involves rapidly mixing a solution of drug in solvent with a solvent-miscible antisolvent; this generates a high supersaturation that induces a fast nucleation rate, leading to the production of nanoparticles. However, it has the inherent problem of scale-up in batch mode due to the challenge of generating a uniformly high supersaturation throughout the large batch volume. The resulting variation of supersaturation throughout the process volume leads to variations in precipitation kinetics, which in turn can influence the final particle size distribution and quality of the product (Zhang et al., 2012; Hadiwinoto et al., 2019). However, performing antisolvent precipitation in continuous mode offers the potential to overcome this problem because the process can be designed to run using volumes small enough to limit the non-uniformity of supersaturation levels. Thus, drug nanoparticle production via continuous antisolvent precipitation not only offers the possibility of process intensification but also offers better control over particle size distribution relative to batch processing (Pandey et al., 2018; D'Addio and Prud'homme, 2011). As such, potential exists to transform current industrial practices by producing drug nanoparticles using continuous antisolvent precipitation.

A thorough search of the pharmaceutical literature for the production of drug nanoparticles via antisolvent precipitation shows that the majority of experimental data were obtained in batch mode (Thorat and Dalvi, 2012; Hu et al., 2011). Very few reports describe the production of nanoparticles via continuous antisolvent precipitation, and of these the drug nanoparticles were often isolated from suspension into the solid-state via coupling the continuous process with spray drying (Dong et al., 2010; Horn and Rieger, 2001; Hu et al., 2011; Dong et al., 2014). However, isolating nanoparticles into the solid-state using complex techniques such as spray drying (and also freeze-drying) can induce

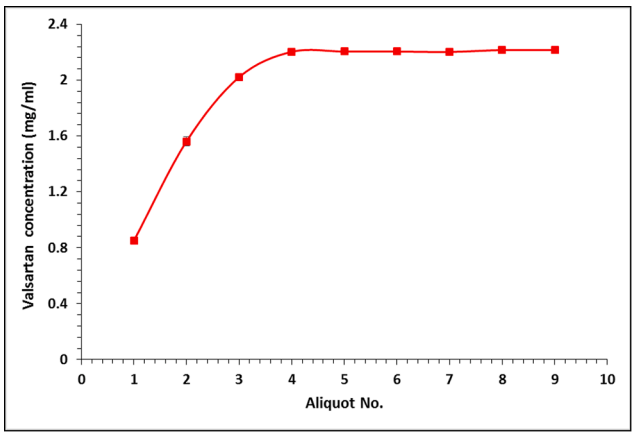

Fig. 2. The concentration of valsartan (mg/mL) in each of the aliquots collected in series. Each aliquot volume corresponds to one residence time of the precipitation chamber (i.e. 60 mL), and the maximum attainable concentration of valsartan is 2.21 mg/mL based on the flow rates of the solvent (valsartan solution) and antisolvent (aqueous solution of Pluronic® F-127).

agglomeration of the nanoparticles due to their high surface energy (Matteucci et al., 2006; Abdelwahed et al., 2006).

Our previous work has described a highly effective way to prepare, stabilise and isolate nanoparticles of a range of poorly water-soluble APIs via a reverse antisolvent precipitation method in batch mode (Kumar et al., 2019; Tierney et al., 2017; Tierney et al., 2015; Bodnar et al., 2017). Indeed, a good understanding of the batch process is almost always required to make a successful design of continuous processes (Jiang and Braatz, 2019). The objective of this work was to develop a semi-continuous antisolvent precipitation process for preparation, stabilization, and isolation of poorly water-soluble drugs with the help of clay carrier particles using an in-house developed semi-continuous system. These clay carrier particles served the dual purpose of stabilizing the nanoparticles in suspension and allowing for their isolation via simple filtration. The process performance was characterized in terms of mixing and total residence times. The product quality was characterized in terms of the particle size distribution of the nanosuspension, percentage isolation, solid-state form, stability of isolated product and dissolution rate by comparing them with batch formulations. The model compound chosen for this study was valsartan (Val), as it was observed in our previous study that Val nanoparticles exhibit good stability when precipitated in batch mode with the help of soluble stabilizers or carrier particles (Kumar et al., 2019). The aim of this study, therefore, was to determine whether Val nanoparticles of similar quality can be prepared, stabilized and isolated in a semi-continuous process. Process variables of antisolvent precipitation such as antisolvent/solvent ratio, flow rate of antisolvent and solvent, residence time and flow rate of suspended carrier particles were optimized to control product quality.

2. Materials and methods

2.1. Materials

Valsartan (Val) ((S)-3-methyl-2-(N-{[2′-(2H-1,2,3,4-tetrazol-5-yl) biphenyl-4-yl]methyl} pentanamido) butanoic acid) was generously supplied by Novartis. Valsartan Form E was prepared from this as-received material according to the procedure outlined in the study published previously by our group (Kumar et al., 2019). Montmorillonite K10 (MMT), Pluronic® F-127, protamine sulphate salt from salmon sperm (PA, a cationic peptide, approx. 5.1 kDa), carboxymethyl cellulose (CMC) and methanol (MeOH) were all purchased from Sigma Aldrich (Ireland) and were used as received without further purification.

2.2. Apparatus and experimental procedure for the preparation of the valsartan nanosuspensions using Pluronic® F-127 as stabilizer in a semi-continuous process

Fig. 1(a) shows the schematic set up for the semi-continuous production of a valsartan nanosuspension via a reverse antisolvent precipitation method. The system consists of two magnetic stirrers, a 60 mL jacketed vessel maintained at 25 °C (precipitation chamber) which was initially filled with 60 mL of an aqueous solution of Pluronic® F-127 (0.2% w/w), a one-liter vessel that contains an aqueous solution of Pluronic® F-127 (0.2% w/w), a collection vial, a peristaltic pump, and a syringe pump (20 mL) containing the drug solution (100 mg Val/mL methanol) in the syringe. During the experiment, the aqueous solution of Pluronic® F-127 (antisolvent) and the valsartan solution in methanol (solvent) were continuously and simultaneously pumped into the precipitation chamber at a fixed flow rate of 50 mL/min and 1.13 mL/min, respectively, Fig. 1(a). These flow rates were selected to achieve the optimum drug solution/anti-solvent ratio in order to obtain the desired particle size distribution of valsartan nanoparticles similar to the batch process. The working volume of the precipitation chamber was 60 mL, which was agitated (800 or 1200 rpm) and overflowed continuously – the overflow was collected as discrete aliquots (60 mL) in a series of numbered vials, Fig. 1(a). The 'residence time' (volume of precipitation chamber/total flow rate) of the continuously forming nanosuspension in the precipitation chamber was 60 mL/51.13 mL.min^{-1} = 1.17 min. The overflow aliquots were collected continuously in series every 1.17 min such that each aliquot volume represented one nominal complete 'residence time' of the precipitation chamber (i.e. 60 mL). At the defined flow rates, the maximum attainable concentration of valsartan in the precipitation chamber (assuming complete desupersaturation) was 2.21 mg/mL.

2.3. Determination of steady-state for the semi-continuous antisolvent precipitation process

The time required to achieve steady-state conditions for the semi-continuous antisolvent precipitation process was defined as the time required to reach the maximum attainable concentration of valsartan (i.e. 2.21 mg/mL) in the precipitation chamber at the defined flow rates of solvent (drug solution) and antisolvent (aqueous solution of Pluronic® F-127). This was determined by analyzing the concentration of valsartan in each aliquot volume (mg/mL) using a Shimadzu UV-1800 UV–Visible spectrophotometer ($\lambda = 250$ nm) after firstly diluting the aliquot volume 40-fold in methanol. The process was deemed to have reached steady state once the valsartan concentration had reached its maximum attainable value (2.21 mg/mL in the precipitation chamber mixture) and thereafter remained at this constant value, from one aliquot to the next.

2.4. Particle Sizing

The particle size distribution of the Pluronic® F-127 stabilized valsartan nanosuspension produced via the semi-continuous antisolvent precipitation process was determined using a Malvern Zetasizer Nano ZSP system with water as the dispersion medium. A refractive index of 1.55 and an absorption index of 0.1 were used to measure the particle size distribution of the valsartan nanoparticles. Each sample was equilibrated for 120 s at 25 °C prior to the measurement. Ten sub-measurements were taken per run and each sample was run in triplicate. The average D_{50} diameter and the standard deviation were recorded for each sample.

The particle size distributions of bare MMT, the Val-MMT nanocomposite suspension and the dried Val-MMT nanocomposite powder were determined by laser diffraction using a Malvern Mastersizer 3000, with water as the dispersion medium. An obscuration rate of 7–9%, a stir speed of 2000 rpm, and pre-measurement delay of 30 s were used for each measurement. A refractive index of 1.55 and an absorption index of

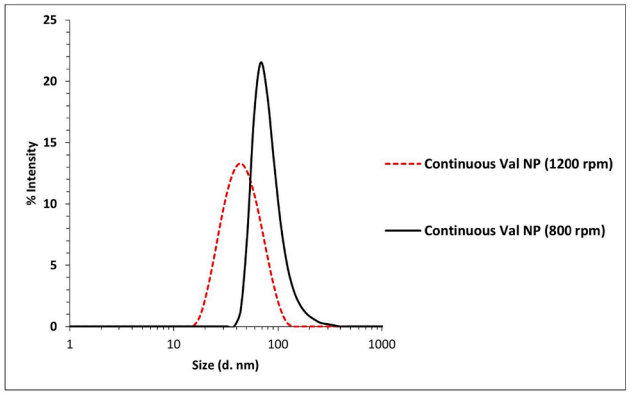

Fig. 3. Particle size distributions of valsartan nanosuspensions at steady state (i.e. after the 4th residence time) following reverse antisolvent precipitation in semi-continuous mode in the presence of Pluronic® F-127 at stirring speeds of 800 and 1200 rpm.

0.1 were used to measure the particle size distribution of the bare MMT and the Val-MMT nanocomposites. Three measurements were taken per run and each sample was run in triplicate. The average D_{50} diameter and the standard deviation were recorded for each sample.

2.5. Apparatus and experimental procedure for the preparation of valsartan-montmorillonite (Val-MMT) and valsartan-protamine functionalised montmorillonite (Val-PA-MMT) nanocomposites via semi-continuous antisolvent precipitation

The production of Val-MMT and Val-PA-MMT nanocomposites (NCs) via semi-continuous antisolvent precipitation was achieved as per the process described in Section 2.2 except that the solution of Pluronic® F-127was replaced by (i) aqueous suspensions of MMT of different concentrations (5 mg/mL to 25 mg/L) agitated at 800 rpm, or (ii) an MMT suspension (5 mg/mL) in an aqueous solution of PA (3 mg PA/g of MMT) agitated at 800 rpm; PA, which is a cationic peptide, was used in our previous study to limit the aggregation of valsartan nanoparticles on MMT carrier particles at high valsartan loadings (Kumar et al., 2019). The collection vial was replaced by a simple Buchner filtration set-up to isolate the Val-MMT or Val-PA-MMT nanocomposites produced at 60 mL aliquot intervals as shown in Fig. 1(b). The isolated nanocomposite materials were dried in a fume hood at ambient temperature and pressure for 24 h. The percentage of Val nanoparticles adsorbed onto the MMT/PA-MMT carrier particles was determined (indirectly) by measuring the concentration of valsartan in the filtrate (i.e. the unadsorbed valsartan) on a Shimadzu UV-1800 spectrophotometer ($\lambda = 250$ nm) by taking an aliquot of the filtrate and diluted by a factor of 10 in methanol to dissolve any drug particles present in the filtrate prior to the measurement. For comparison purpose, Val-MMT/Val-PA-MMT NCs at different valsartan loadings (% w/w) were also prepared in a batch experiment according to the procedure outlined in the study published previously by our group (Kumar et al., 2019).

2.6. Powder X-ray diffraction (PXRD)

Reflection powder X-ray diffractograms (PXRDs) were recorded using an Empyrean diffractometer (PANalytical, Phillips) with Cu $K\alpha_{1,2}$ radiation ($\lambda = 1.5406$ Å) operating at 40 kV and 40 mA at room temperature. Samples were scanned from 5 to 50° (2θ) with 0.026° 2θ/min step size and 112.97 s per step, on a flat stage that was spinning at 4 rpm.

2.7. Differential Scanning Calorimetry (DSC)

Differential Scanning Calorimetry (DSC) was carried out using a PerkinElmer instrument Pyris 1 DSC in the range 30–170 °C at a scan rate of 10 °C/min under a nitrogen environment (30 mL/min). Experiments were carried out using platinum pans with pinholes (as manufactured), sealed by a crimping press. The instrument was calibrated using samples of indium and lead.

2.8. Solid-state nuclear magnetic resonance (SSNMR)

^{13}C SSNMR cross-polarization magic-angle spinning (CPMAS) spectra were collected with a Bruker Avance III HD NMR spectrometer, operating at 400.23 and 100.63 MHz, for ^{1}H and ^{13}C respectively. Dry powdered samples were packed without further preparation into cylindrical zirconia rotors with a 4 mm o.d. and an 80 µL volume. The ^{13}C CPMAS spectra were acquired at room temperature at a spinning speed of 12 kHz, using a ramp cross-polarization pulse sequence with a 90° ^{1}H pulse of 3 µs, a contact time of 3 ms, an optimized recycle delay of 3.14 s and a number of scans included in the range 400–26900, depending on the sample. A two-pulse phase modulation (TPPM) decoupling scheme was used, with a radiofrequency field of 69.4 kHz. The ^{13}C chemical shift scale was calibrated through the low field peak signal of an external standard, adamantane (at 38.48 ppm).

2.9. Tableting

The greater productivity of the semi-continuous method (compared with the batch method) allowed a small number of tablets to be formulated and tabletted. Dried Val-MMT/Val-PA-MMT nanocomposite solids with various Val loadings (% w/w) were tabletted with a compaction simulator (Gamlen Tableting D series) using a 6 mm round and flat-faced punch and die set. Two formulations were made; the first

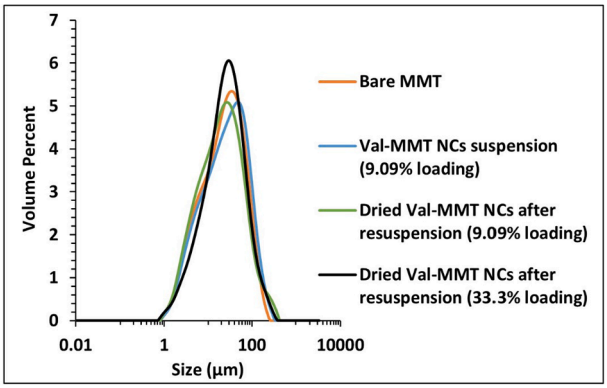

Fig. 4. Particle size distribution of bare and valsartan loaded MMT before and after filtering and drying.

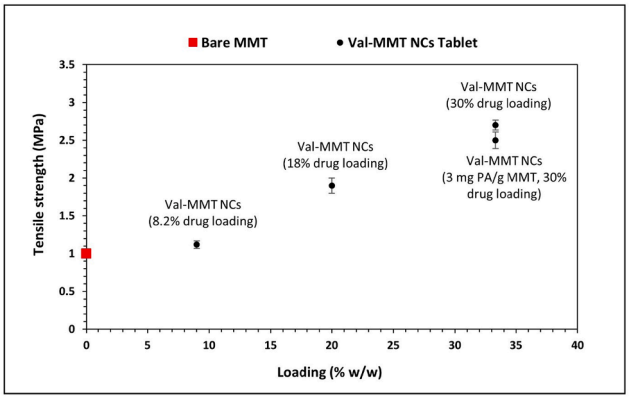

Fig. 5. Tensile strength of bare MMT and Val-MMT/Val-PA-MMT NCs tablets at different valsartan loadings (% w/w) compressed at a load of 300 kg, n = 3.

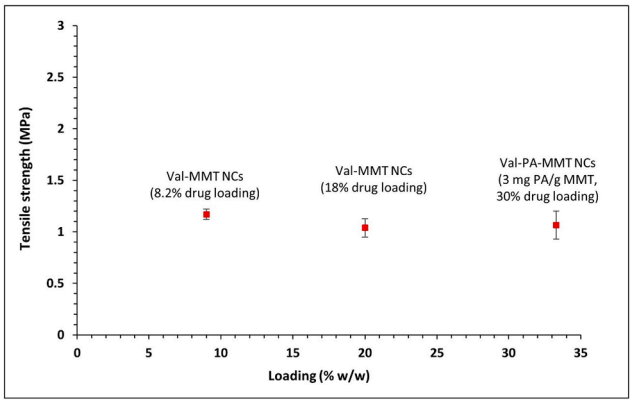

Fig. 6. Tensile strength of Val-MMT NC tablets at 8.2% and 18% w/w valsartan loadings and Val-PA-MMT NC tablets at 30% w/w valsartan loading (3 mg PA/g MMT), compacted at loads of 300, 200 and 160 kg respectively, n = 3.

formulation contains only Val-MMT/Val-PA-MMT NCs while the second formulation comprised a blend of Val-MMT/Val-PA-MMT NCs and CMC (10% w/w) as disintegrant. For each compression, 100 mg of sample (100 mg Val-MMT/Val-PA-MMT NCs or 100 mg sample containing 90% w/w Val-MMT/Val-PA-MMT NCs and 10% w/w CMC as disintegrant) was manually filled into the die and compacted by applying loads of 160 to 300 kg at a controlled upper punch velocity of 1 mm s^{-1}. Load displacement data were used to calculate detachment and ejection stresses using in-die Heckle analysis. The tablet crushing force, hardness (F), thickness (h), diameter (D), and weight of the tablets produced were determined using a PTB 311E pharm test hardness tester. The tablet tensile strength, σ_t (MPa), was calculated using Eq. (1) (Fell and Newton, 1970)

$$\sigma_t = \frac{2F}{\pi D h} \tag{1}$$

where F = hardness (N), h = tablet thickness (mm) and D = tablet diameter (mm).

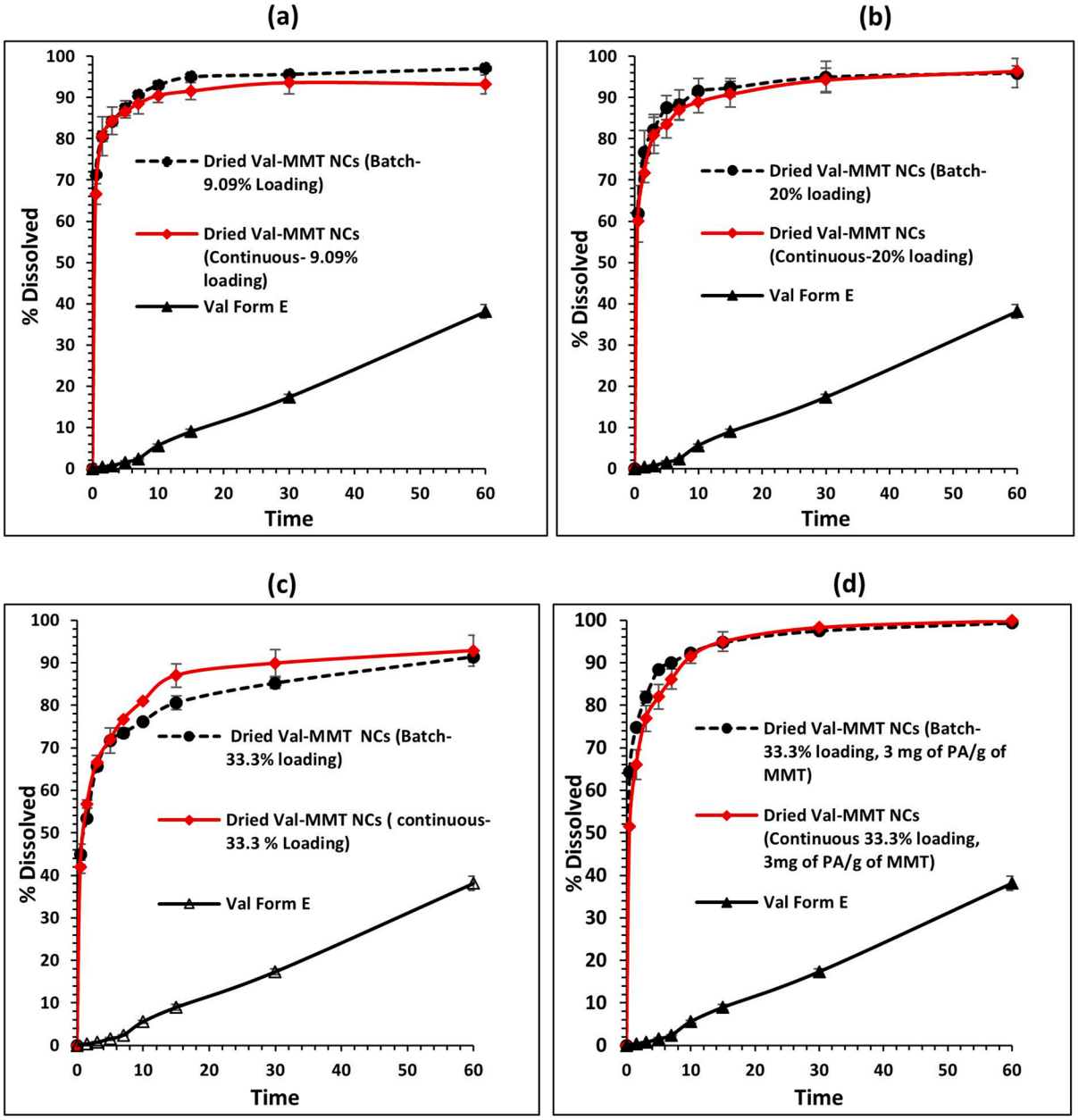

Fig. 7. Comparison of the dissolution profile of Val Form E (~11 μm) with those of dried Val-MMT nanocomposite powders prepared in the batch experiment and dried Val-MMT nanocomposite powders prepared in the semi-continuous experiment at different valsartan loadings: (a) 9% w/w loading, (b) 20% w/w loading, (c) 33.3% w/w loading and (d) 33.3% loading, 3 mg PA/g MMT.

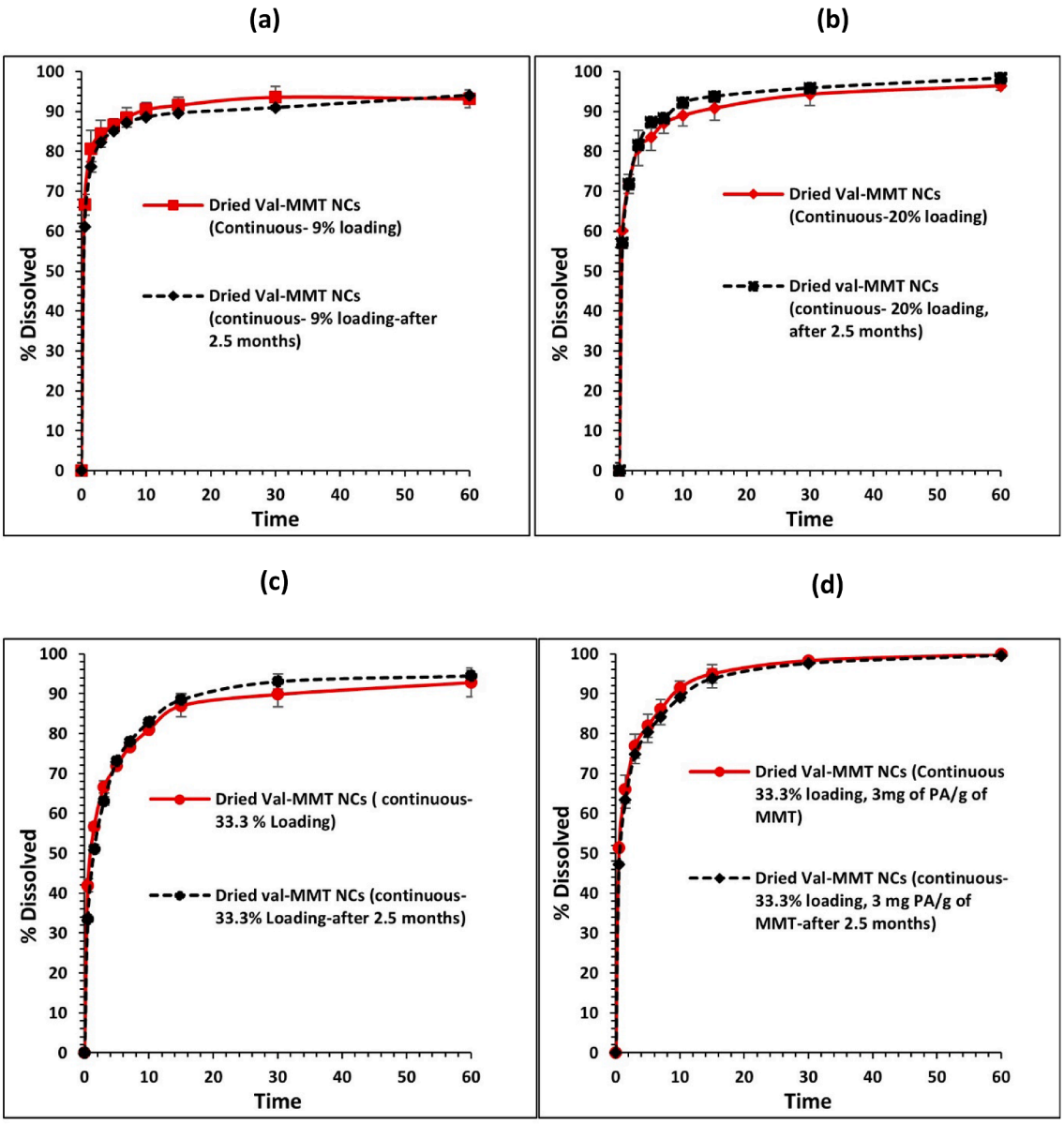

Fig. 8. Comparison of the dissolution profile of fresh dried Val-MMT nanocomposites prepared in the semi-continuous experiment with those of aged Val-MMT nanocomposites prepared in the semi-continuous experiment (samples stored for 2.5 months in an accelerated humidity chamber at 40 °C and 75% relative humidity) at different valsartan loadings: (a) 9% w/w loading, (b) 20% w/w loading, (c) 33.3% w/w loading and (d) 33.3% loading, 3 mg of PA/g MMT.

Tensile strength in excess of 1 MPa is usually desirable for tablets (Schmidtke et al., 2017).

2.10. *In vitro* drug release studies

In vitro drug release studies of (i) valsartan Form E and (ii) dried powders of Val-MMT/Val-PA-MMT NCs at different valsartan loadings ranging from 9 to 33.3% w/w were carried out in sink conditions in 100 mL deionized water under continuous agitation (300 rpm) at 37 ± 0.5 °C. The extent of drug dissolution was measured using a Shimadzu UV-1800 UV–Visible spectrophotometer at λ = 250 nm by withdrawing 1 mL aliquots at pre-determined time intervals (0.5, 1.5, 3, 5, 10, 15, 30, 45 and 60 min) from the bulk solution with a preheated plastic syringe and filtering through 0.22 μm pore preheated PTFE syringe filters. All measurements were carried out in triplicate.

In vitro drug release studies of the tablet formulation of Val-MMT/Val-PA-MMT NCs and powdered formulation composed of a physical mix of Val-MMT/Val-PA-MMT NCs and CMC were carried out using a USP compliant tablet dissolution type II (Pharma Test PTWS 120D) paddle apparatus. They were carried out in sink conditions in 900 mL deionized water at 37 ± 0.5 °C at a paddle rotation of 150 rpm. One mL aliquots were withdrawn at predetermined time intervals and the amount of valsartan released was determined via UV-1800 UV–Visible spectrophotometer as described above. All measurements were carried out in triplicate.

2.11. *Accelerated stability tests*

To investigate the stability of the nanocomposites over time, samples of Val-MMT and Val-PA-MMT NCs (all in dry solid form) were exposed to 40 °C and 75% relative humidity for 2.5 months in a closed desiccator containing a supersaturated solution of NaCl. After 2.5 months, the samples were analysed via DSC, PXRD and SSNMR, and *in vitro* drug release studies were also performed, to determine whether the material had changed through recrystallization or agglomeration.

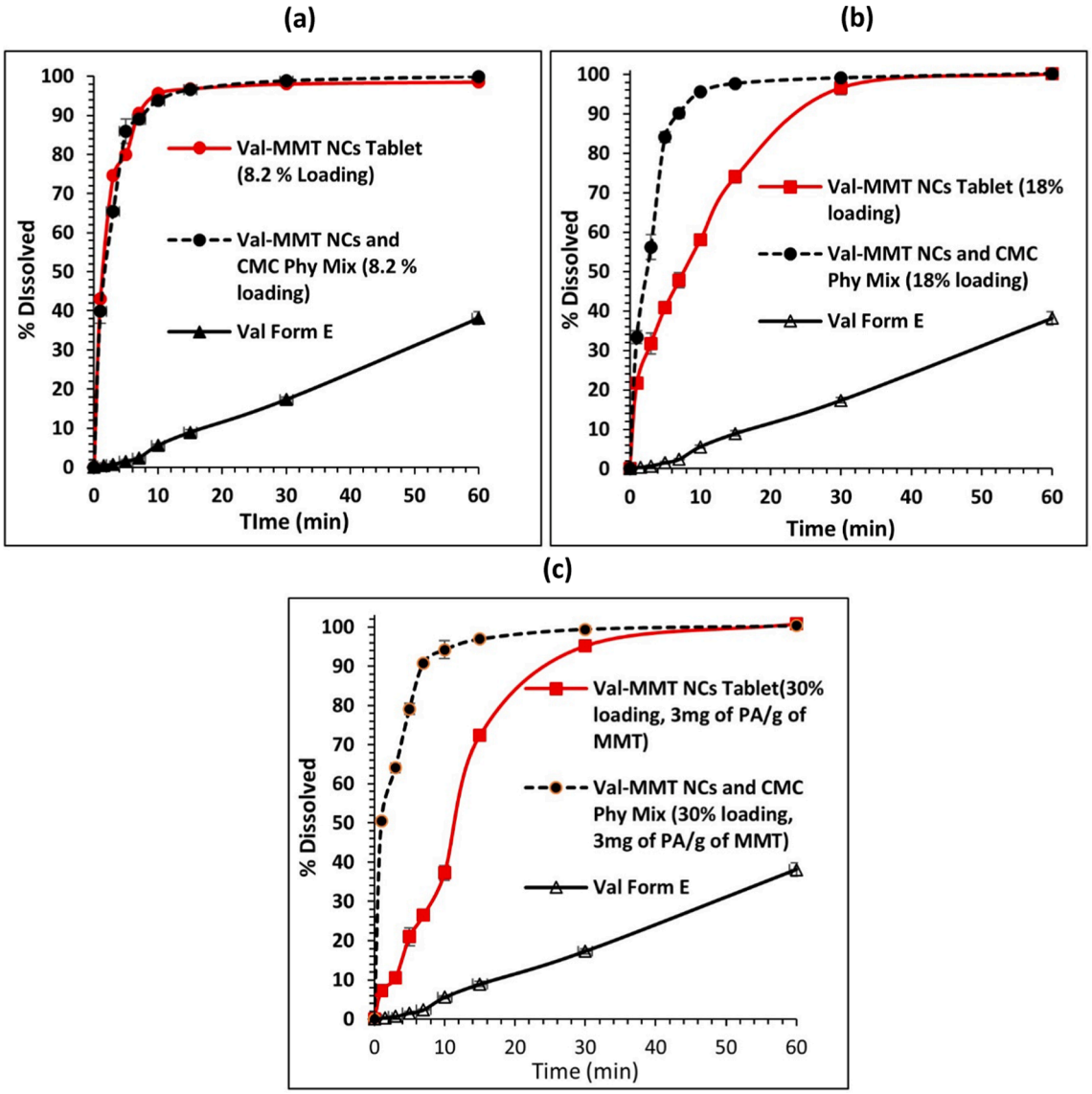

Fig. 9. Comparison of the dissolution profile of Val Form E (~11 μm) with those for valsartan from a selection of powdered samples and tablet formulations at different valsartan loadings (% w/w) and where the formulations comprised a 90:10 w/w blend of Val-MMT or Val-PA-MMT NCs and CMC as disintegrant: (a) powdered sample composed of a physical mix of Val-MMT NCs and CMC (Val loading = 8.2% w/w), and Val-MMT NCs tablet (Val loading = 8.2% w/w, tensile strength = 1.1 MPa), (b) powdered sample composed of a physical mix of Val-MMT NCs and CMC (Val loading = 18% w/w), and Val-MMT NCs tablet (Val loading = 18% w/w, tensile strength = 2 MPa), and (c) powdered sample composed of a physical mix of Val-PA-MMT NCs and CMC (Val loading = 30% w/w, 3 mg PA/g MMT), and Val-PA-MMT NCs tablet (Val loading = 30% w/w, 3 mg PA/g MMT, tensile strength = 2.6 MPa); n = 3.

3. Results and discussion

3.1. Steady-state measurement

At the studied flow-rates, one nominal complete 'residence time' of the precipitation chamber (i.e. 60 mL) took 1.17 min to collect as a discrete aliquot, as discussed in Section 2.2. Also, the maximum attainable concentration of valsartan in the precipitation chamber was 2.21 mg/mL. As such, steady state conditions were deemed achieved once the valsartan concentration had reached 2.21 mg/mL in the precipitation chamber mixture and thereafter remained at this constant value from one discrete collected aliquot to the next. On this basis, the system was found to achieve steady state operation after four 'residence times', which equated to the collection of four aliquots over ca. 5 min (4 residence times × 1.17 min/residence time). Thereafter the semi-continuous system operated robustly for the entire duration of the experiment (~16 min), Fig. 2. At these flow rates, ~3 L of nanosuspension can be produced per hour, and while the single-injection system used here limited the duration of the experiment, a parallel syringe injection system would allow for longer running times.

3.2. Particle size distribution of polymer stabilized nanosuspensions from the semi-continuous preparation

Rapid mixing during antisolvent precipitation is necessary to generate small particles and narrow particle size distributions (Thorat and Dalvi, 2012). The steady-state particle size distribution of valsartan nanoparticles stabilized by Pluronic® F127 changes from 68 ± 7 nm to 51 ± 1 nm as the stirring speed increased from 800 to 1200 rpm in the precipitation chamber, Fig. 3. Thus rapid mixing appears to generate a more homogeneous solution, with a uniformly high supersaturation, which results in faster nucleation rates generating smaller particle sizes. The particle size distribution at 800 rpm was not as narrow as that obtained during the batch experiment in which the particle size of 50 ± 0.4

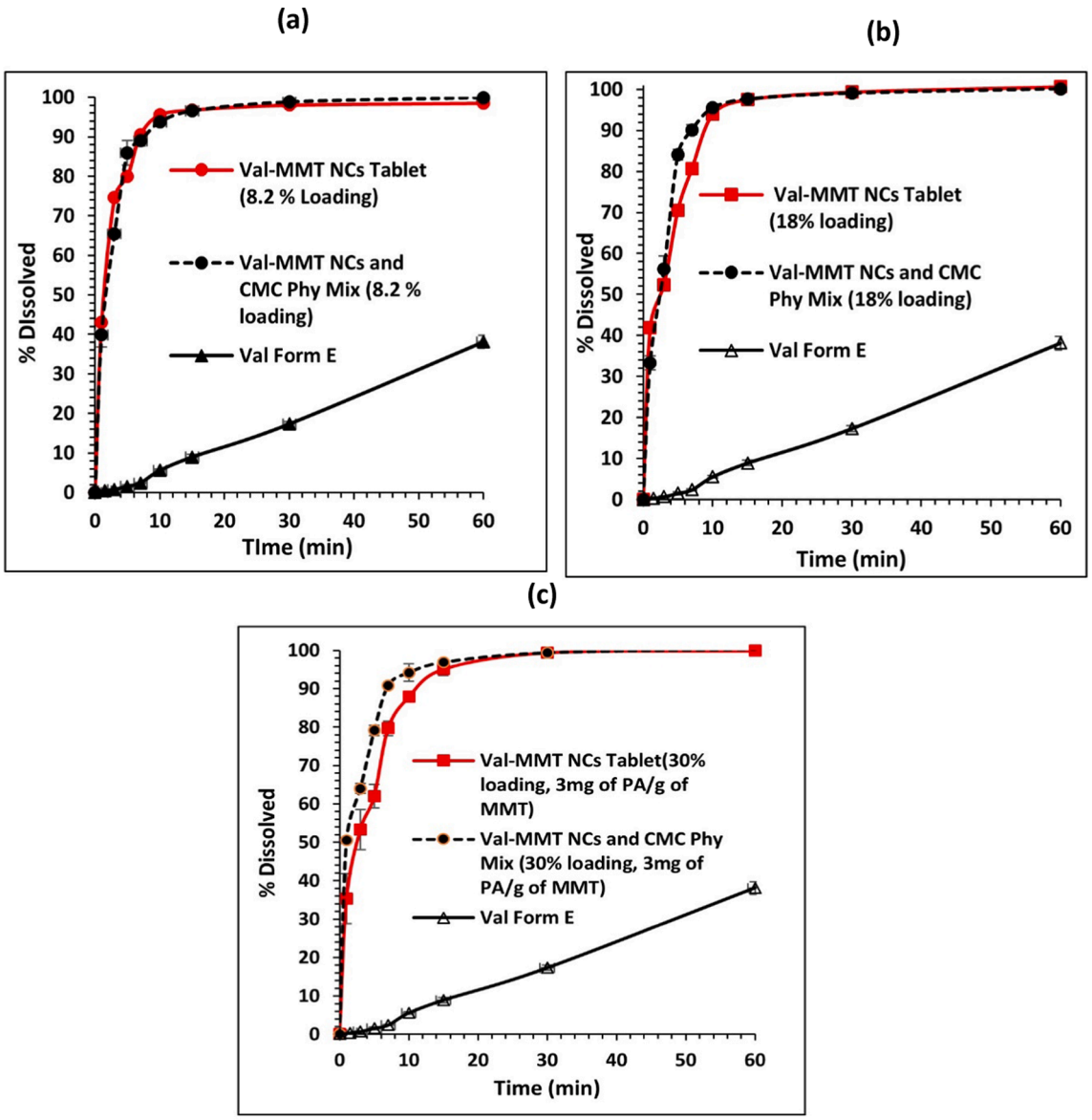

Fig. 10. Comparison of the dissolution profile of Val Form E (~11 μm) with those for valsartan from a selection of powdered samples and tablet formulations at different valsartan loadings (% w/w) and where the formulations comprised a 90:10 w/w blend of Val-MMT or Val-PA-MMT NCs and CMC as disintegrant: (a) powdered sample composed of a physical mix of Val-MMT NCs and CMC (Val loading = 8.2% w/w), and Val-MMT NCs tablet (Val loading = 8.2% w/w, tensile strength = ~1 MPa), (b) powdered sample composed of a physical mix of Val-MMT NCs and CMC (Val loading = 18% w/w), and Val-MMT NCs tablet (Val loading = 18% w/w, tensile strength = ~1 MPa), and (c) powdered sample composed of a physical mix of Val-PA-MMT NCs and CMC (Val loading = 30% w/w, 3 mg PA/g MMT), and Val-PA-MMT NCs tablet (Val loading = 30% w/w, 3 mg PA/g MMT, tensile strength = ~1 MPa); n = 3.

nm was obtained with very narrow particle size distribution at 800 rpm (Kumar et al., 2019). However, when the stirring was increased to 1200 rpm, the particle size distribution obtained during the semi-continuous process was similar to the batch particle size distribution at 800 rpm, Fig. 3. This can be attributed to the different level of mixing that is required when comparing the batch experiment with the semi-continuous. All subsequent semi-continuous studies were therefore conducted at the optimized stirring speed of 1200 rpm.

3.3. Attachment of valsartan nanoparticles onto MMT/PA-MMT carrier particles during the semi-continuous process

In our previous study, almost complete adsorption (>99%) of valsartan nanoparticles onto MMT or PA-MMT carrier particles was observed using the batch process (Kumar et al., 2019). The attachment of Val nanoparticles to MMT/PA-MMMT carrier particles during the semi-continuous process was confirmed by the clear filtrate obtained in each aliquot and by checking the concentration of valsartan in the filtrate by UV–Vis analysis. The concentration of valsartan in the filtrate confirmed that almost all of the valsartan present had adsorbed onto the MMT/PA-MMT carrier particles (>99%). Thus it can be said that this semi-continuous system is successful in preparing and isolating drug nanoparticles in the solid-state in which > 99% of the drug nanoparticles are adsorbed onto the carrier particles.

The particle size distributions of the bare MMT, 9.09% w/w valsartan loaded Val-MMT nanocomposites suspension, 9.09% w/w dried valsartan loaded Val-MMT nanocomposites and 33.3% w/w dried valsartan loaded Val-MMT nanocomposites were found to be the same (at 26.0 ± 0.5, 26.3 ± 0.4, 25.5 ± 1.5 and 26 ± 2 μm respectively, Fig. 4).

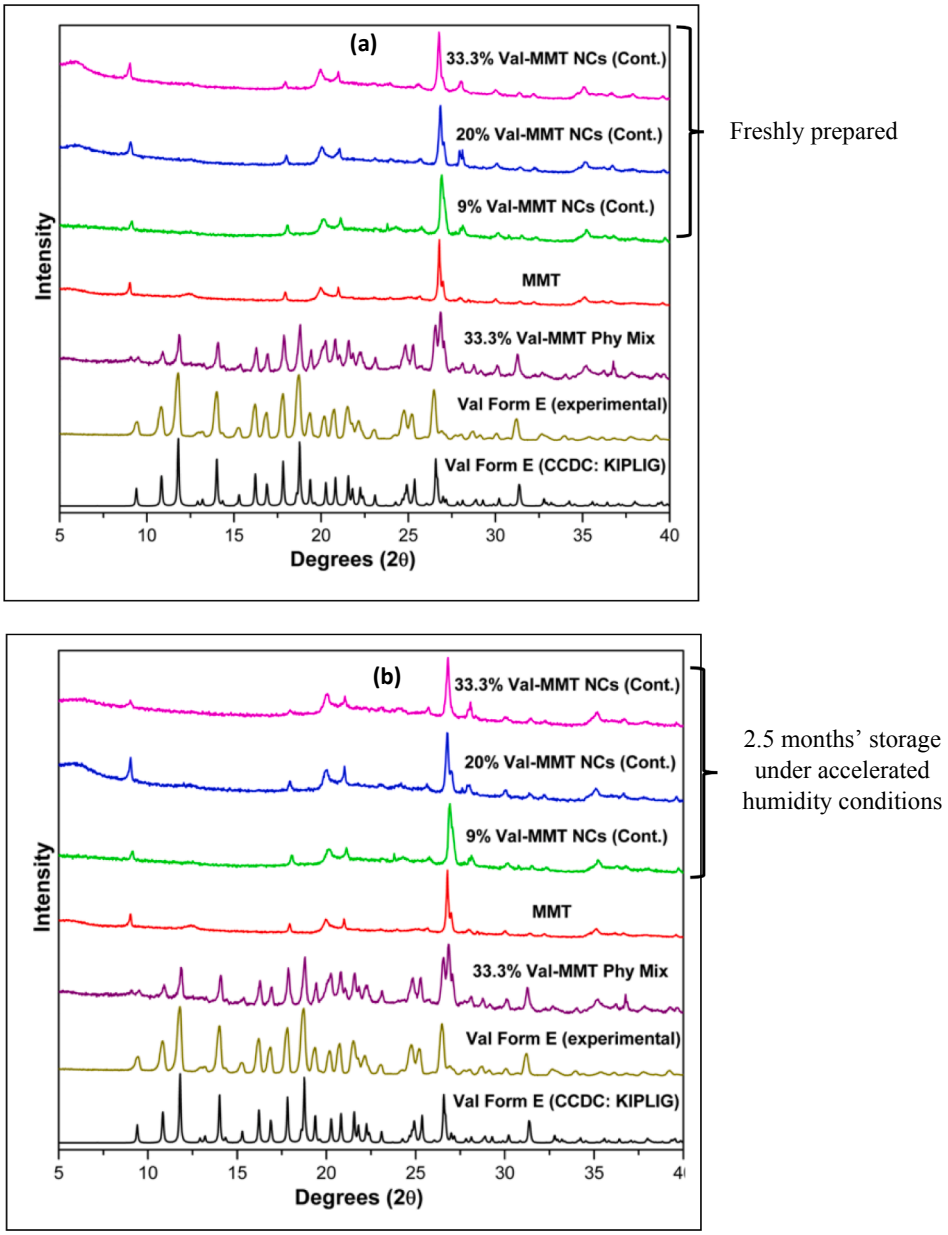

Fig. 11. PXRD patterns of valsartan Form E (experimental and from the CSD), a 33.3% w/w physical mixture of valsartan Form E and MMT, MMT and a selection of Val-MMT nanocomposites with different valsartan loadings (% w/w) produced via the semi-continuous method: (a) freshly prepared Val-MMT nanocomposites and (b) aged Val-MMT nanocomposites (2.5 months' storage under accelerated humidity conditions).

3.4. Tableting of Val-MMT nanocomposites

Solid Val-MMT NC products obtained from semi-continuous experiments were compressed to assess the tableting behaviour of Val-MMT/Val-PA-MMT NCs at various Val loadings (% w/w). These tablets' tensile strength was observed to increase with an increase in valsartan loading in the Val-MMT NCs Fig. 5. This was probably due to an increase in cohesive interparticulate forces (such as mechanical interlocking, Van der Waals forces, etc.) arising from an increase in the nanoparticle surface area available for contact and cohesion during tableting at higher loadings of valsartan nanoparticles (Eichie and Kudehinbu, 2009; Cabiscol et al., 2020; Virtanen et al., 2010). A tensile strength in excess of 1 MPa is usually desirable for tablets (Schmidtke et al., 2017). The tensile strength of all the tablets with different valsartan loadings exceeded this limit, thus yielding robust tablets without any use of other excipients, Fig. 5 (Schmidtke et al., 2017; Pitt and Heasley, 2013). While this finding is specific to valsartan, it demonstrates the potential of nanocomposites produced via this semi-continuous approach to be directly compressed into tablets without the need to use other excipients. The tablets produced were composed only of the nanocomposite material and 10% w/w disintegrant (CMC). Thus, the drug loading in the tablets was slightly below that of the drug loading in the nanocomposite materials; for example, 33.3% w/w/ drug loaded nanocomposite yielded tablets with a 30% w/w drug loading. The tensile strength of Val-MMT/Val-PA-MMT NC tablets at different valsartan loadings was kept similar by compressing the 9% and 20% w/w loaded Val-MMT NCs and the 33.3% w/w loaded Val-PA-MMT NC (3 mg PA/g MMT) tablets at compression loads of 300, 200 and 160 kg respectively Fig. 6.

3.5. Dissolution studies of Val-MMT nanocomposites powders produced via the semi-continuous method

Fig. 7 shows the dissolution behaviour of Val-MMT NC powders with 9%, 20% and 33.3% w/w valsartan loadings and Val-PA-MMT NC

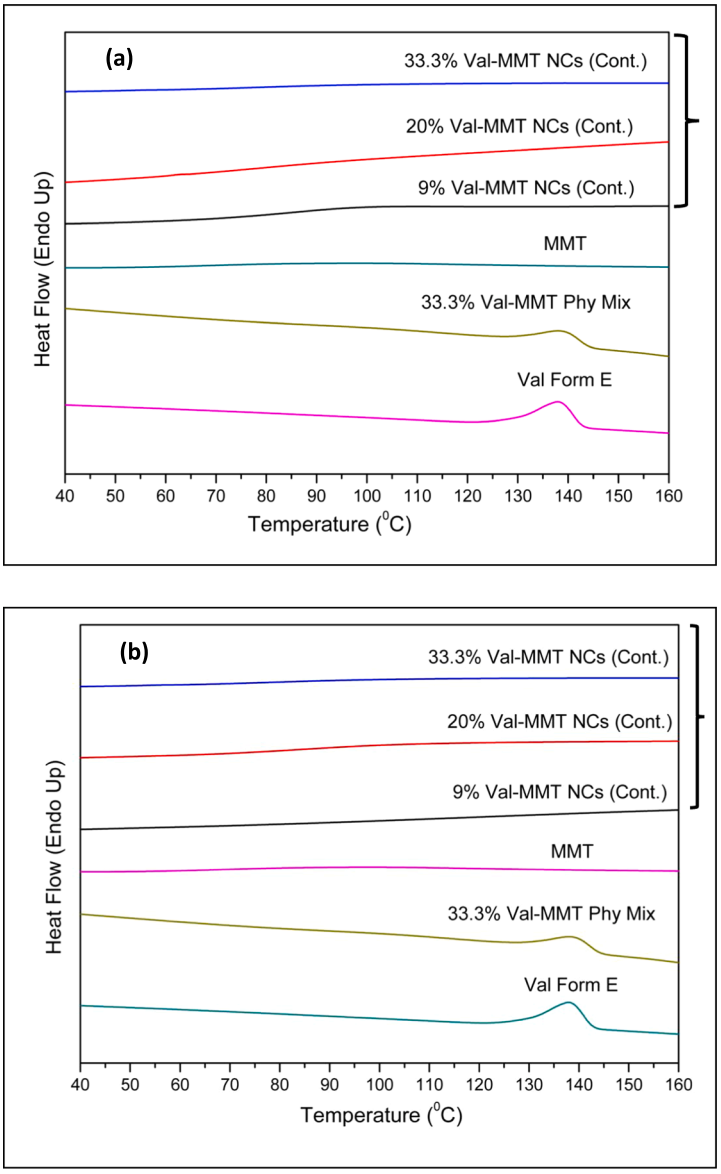

Fig. 12. DSC thermograms of valsartan Form E, a 33.3% w/w physical mixture of valsartan Form E and MMT, MMT and a selection of Val-MMT nanocomposites with different valsartan loadings (% w/w): (a) freshly prepared Val-MMT nanocomposites and (b) aged Val-MMT nanocomposites (2.5 months' storage under accelerated humidity conditions).

powder at 33.3% w/w valsartan loading (3 mg PA/g of MMT). For comparison purposes, this figure also includes the dissolution of Val-MMT NCs at different valsartan loading (w/w) (9%, 20%, 33.3% and 33.3% loading, 3 mg PA/g of MMT) prepared in a batch experiment and Val Form E powder. The dissolution behaviour of Val-MMT nanocomposites produced in the semi-continuous method was found to be comparable with those prepared in the batch experiments, and they dissolved much faster than the larger particle sized crystals of Val Form E (~11 μm), Fig. 7. Thus the semi-continuous method of preparing, stabilizing and isolating valsartan nanoparticles is on a par with the batch method in terms of dissolution behaviour.

3.6. Stability of Val-MMT/Val-PA-MMT nanocomposites powders

After storage for 2.5 months under accelerated humidity conditions, Val-MMT and Val-PA-MMT nanocomposites displayed valsartan dissolution profiles comparable with those of freshly prepared Val-MMT and Val-PA-MMT nanocomposites, Fig. 8. This indicates that no recrystallization/polymorphic transformation/aggregation of the valsartan nanoparticles had occurred during this time. Thus, the Val-MMT/Val-PA-MMT nanocomposites produced via this semi-continuous process possessed a shelf-life stability equivalent to > 10 months (based on the accelerated stability storage conditions of 40 °C and 75% relative humidity for 2.5 months), Fig. 8.

3.7. Dissolution studies of Val-MMT nanocomposites tablets

The tablet (100 mg) formulation used for dissolution studies comprised a 90:10 w/w blend of Val-MMT or Val-PA-MMT NCs and CMC as disintegrant. The dissolution profiles of valsartan from tablets at different valsartan loadings are presented in Figs. 9 and 10; the stated valsartan loadings take into account the presence of 10% (w/w) CMC in the formulation. The dissolution profile of valsartan from the tablets was found to deteriorate as the valsartan loading in the tablets increased (Fig. 9). This appears to correlate with the increase in tensile strength of the tablets as the valsartan loading increases (discussed in Section 3.4). To minimise the effect of the tablets' varying tensile strength on dissolution behaviour, 90:10 w/w blends of Val-MMT or Val-PA-MMT NCs

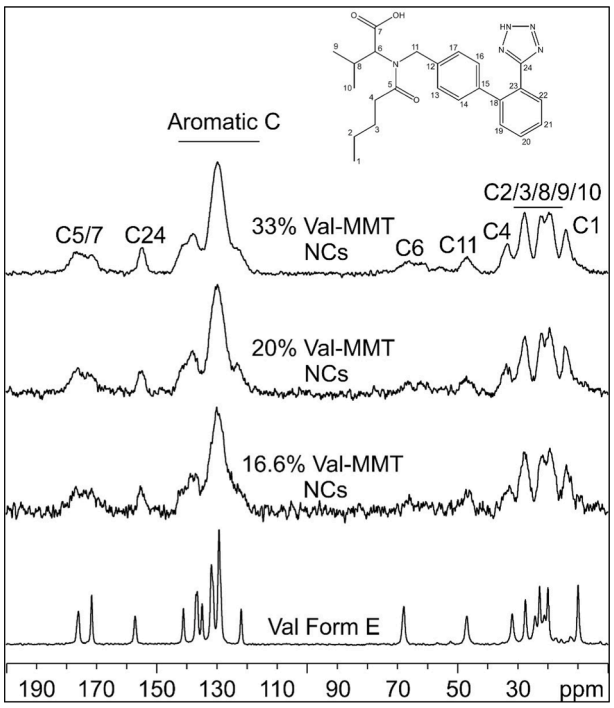

Fig. 13. ^{13}C (100 MHz) CPMAS spectra of Val Form E and freshly prepared Val-MMT NCs (16.6%, 20% and 33% w/w loadings), acquired at a spinning speed of 12 kHz at room temperature.

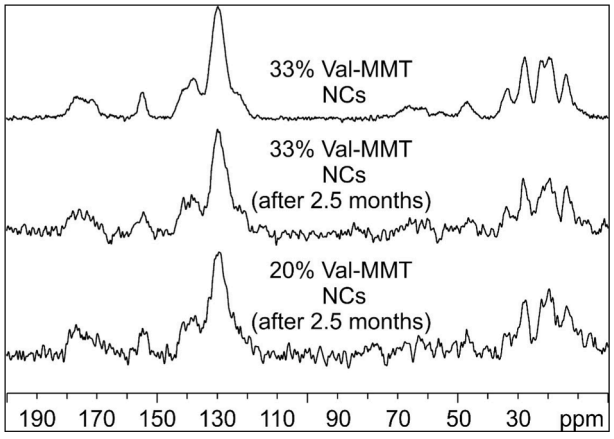

Fig. 14. ^{13}C (100 MHz) CPMAS spectra of aged Val-MMT NCs (20% and 33% w/w loadings) after 2.5 months' storage under accelerated humidity conditions and freshly prepared Val-MMT NC (33% w/w loading), acquired at a spinning speed of 12 kHz at room temperature.

and CMC at different valsartan loadings were compressed to different compression loads in order to form tablets of a similar tensile strength (~1 MPa) for dissolution studies (discussed in Section 3.4). The dissolution profiles of valsartan from the resulting tablet formulations were comparable with those of the corresponding powdered physical mix samples of Val-MMT NCs and CMC as illustrated in Fig. 10. Hence, the tableting of Val-MMT nanocomposites powder does not adversely affect the dissolution profile once the tablet compression load has been tuned accordingly to control the tensile strength. In principle, therefore, API-MMT nanocomposites obtained from this semi-continuous process can be readily compressed into tablets without compromising the dissolution behaviour of the APIs.

3.8. Solid state characterization

PXRD patterns were compared for Val Form E, a 33.3% w/w physical mixture of Val Form E and MMT, MMT, and variously valsartan-loaded Val-MMT NCs produced via the semi-continuous process (freshly prepared samples (Fig. 11(a)) and samples following 2.5 months' storage under accelerated humidity conditions (Fig. 11(b))). No characteristic valsartan diffraction peaks were observed in any of the variously valsartan-loaded Val-MMT nanocomposites, thus confirming the X-ray amorphous nature of the valsartan in the fresh samples and the samples stored for 2.5 months under accelerated humidity conditions. DSC thermograms were compared for Val Form E, a 33.3% w/w physical mixture of Val Form E and MMT, MMT, and variously valsartan-loaded Val-MMT NCs produced via the semi-continuous process (freshly prepared samples (Fig. 12(a)) and samples following 2.5 months' storage under accelerated humidity conditions (Fig. 12(b))) to further investigate the physical state of valsartan in the Val-MMT nanocomposites. The thermogram of unprocessed Val Form E showed an endothermic peak at 138.4 ± 0.4 °C corresponding to its melting temperature, as did the thermogram of its 33.3% w/w physical mixture with MMT. However, a melting peak was not detected in any of the thermograms of the variously valsartan-loaded Val-MMT nanocomposite samples, suggesting that the adsorbed valsartan nanoparticles therein were amorphous when freshly produced and did not undergo a crystalline transformation during 2.5 months' storage under accelerated humidity conditions, Fig. 12(a) and (b).

3.9. Solid-state nuclear magnetic resonance (SSNMR) of Val-MMT nanocomposites

Solid-state NMR (SSNMR) has established itself as a complementary technique to X-ray diffraction in the study of solid materials, especially in the case of APIs (Chierotti and Gobetto, 2008; Bordignon et al., 2017; Rossi et al., 2018; Geppi et al., 2008; Veinberg et al., 2016). Indeed, contrary to solution NMR, SSNMR does not require the dissolution of the sample to be analyzed, thus avoiding the loss of any feature intimately connected with its structure in the solid-state. It can provide precious information about poorly crystalline or even amorphous samples (Lu et al., 2019; Agrawal et al., 2004). Moreover, thanks to its high sensitivity to the local environment of the observed nuclei, SSNMR can be employed to probe the effects of surface interactions on the materials of interest (Vogt et al., 2013; Paudel et al., 2014). ^{13}C cross-polarization magic-angle spinning (CPMAS) spectra were acquired for crystalline Val Form E, freshly prepared Val-MMT NCs with different valsartan loadings (16.6%, 20% and 33% w/w) and aged Val-MMT NCs (20% and 33% w/w loading) following 2.5 months' storage under accelerated humidity conditions. This allowed the physical state of the valsartan in freshly prepared and aged Val-MMT nanocomposites to be evaluated. Fig. 13 shows the ^{13}C CPMAS spectra of Val Form E and the freshly prepared Val-MMT NCs.

When compared with the signals in the spectrum for crystalline Val Form E, the signals in the spectra for the three Val-MMT nanocomposites are consistent with the presence of Val. The resonances in the three Val-MMT NCs spectra are consistently broader than those for crystalline Val Form E, with an average full width at half maximum value of about 350 Hz for the Val-MMT NCs spectra versus about 90 Hz for Val Form E. This is due to a loss of crystallinity of valsartan in the Val-MMT NCs, suggesting that the adsorbed valsartan nanoparticles thereon are amorphous. This was confirmed by comparing the spectra for the Val-MMT nanocomposites with that for amorphous valsartan reported by Skotnicki *et al.* in 2016 (Skotnicki et al., 2016) (not shown). The spectra of the three freshly prepared Val-MMT NCs at different Val loadings in Fig. 13 are superimposable on each other, indicating that the valsartan is not meaningfully affected by different interactions in the three materials as its loading on MMT varies. Above the spectra in Fig. 13, valsartan's chemical structure is shown, with C atoms numbered to clarify the

proposed assignments of the related ^{13}C solid-state NMR resonances. Fig. 14 represents a stack of the ^{13}C CPMAS spectra for the two aged Val-MMT NC samples (samples were stored for 2.5 months in the accelerated testing humidity chamber) and the freshly prepared 33% w/w loaded Val-MMT NC sample. As in the previous figure, the three spectra are superimposable, suggesting that the 2.5 months' storage under accelerated humidity conditions does not alter the physical state of valsartan in the Val-MMT nanocomposites. This confirms the excellent humidity stability of Val-MMT nanocomposites with an ambient shelf life of $>$ 10 months (based on the accelerated stability storage conditions of 40 °C and 75% relative humidity for 2.5 months).

4. Conclusion

An experimental study was conducted to develop a semi-continuous and scalable process to prepare, stabilize and isolate valsartan (Val) nanoparticles. The reverse anti-solvent precipitation method combined with the capture and stabilization of the Val nanoparticles by montmorillonite (MMT) or protamine (PA) functionalised MMT lends itself readily to semi-continuous operation whereby gram scale quantities of Val-MMT/Val-PA-MMT nanocomposites are readily produced at a nominal reactor scale of 60 mL. The in-house developed semi-continuous system operated robustly for the full duration of all experiments (~16 min) and steady-state conditions were reached within ~ 5 min. The dissolution profiles of the resulting Val-MMT/Val-PA-MMT nanocomposite powders were comparable with those of the corresponding Val-MMT/Val-PA-MMT nanocomposite powders produced via batch processing. Furthermore, the dissolution profiles of tablets formulated from a 90:10 w/w blend of the Val-MMT/Val-PA-MMT nanocomposite powders with CMC (as a disintegrant) were comparable with those of the corresponding physical mixtures up to the highest tested valsartan loading of 33.3% w/w, once the tablet compression loads had been tuned accordingly to control the tensile strength. According to PXRD, DSC and SSNMR data, the Val-MMT nanocomposites were amorphous and have a shelf life stability equivalent to $>$ 10 months (based on their observed stability up to 2.5 months under accelerated testing conditions of 40 °C and 75% relative humidity). Thus, the developed semi-continuous process in this study offers a rapid and robust template for preparing stable API nanosuspensions, which can then be readily isolated via adsorption (at different API loadings) onto inert carrier particles. The resulting API-carrier particle nanocomposite solids are suitable for tableting, affording fast-dissolving tablets for oral dosage forms.

CRediT authorship contribution statement

Ajay Kumar: Conceptualization, Methodology, Writing - original draft. **Kiran A. Ramishetty:** Methodology. **Simone Bordignon:** Methodology, Investigation. **Benjamin K. Hodnett:** Conceptualization, Supervision, Writing - review & editing. **Peter Davern:** Conceptualization, Supervision, Writing - review & editing. **Sarah Hudson:** Conceptualization, Supervision, Writing - review & editing.

Declaration of Competing Interest

The authors declare that they have no known competing financial interests or personal relationships that could have appeared to influence the work reported in this paper.

Acknowledgements

This publication has emanated from research conducted with the financial support of the Synthesis and Solid State Pharmaceutical Centre, funded by Science Foundation of Ireland (SFI) under grant numbers 12/RC/2275_P2 and 15/US-C2C/13133, as well as support from the Bernal Institute and the Department of Chemical Sciences at the University of Limerick.

References

Abdelwahed, W., Degobert, G., Stainmesse, S., Fessi, H., 2006. Freeze-drying of nanoparticles: formulation, process and storage considerations☆. Adv. Drug Deliv. Rev. 58 (15), 1688–1713.

Agrawal, S., Ashokraj, Y., Bharatam, P.V., Pillai, O., Panchagnula, R., 2004. Solid-state characterization of rifampicin samples and its biopharmaceutic relevance. Eur. J. Pharm. Sci. 22 (2–3), 127–144.

Bodnar, K., Hudson, S.P., Rasmuson, Å.C., 2017. Stepwise use of additives for improved control over formation & stability of mefenamic acid nanocrystals produced by antisolvent precipitation. Cryst. Growth Des. 17 (2), 454–466.

Bordignon, S., Cerreia Vioglio, P., Priola, E., Voinovich, D., Gobetto, R., Nishiyama, Y., Chierotti, M.R., 2017. Engineering codrug solid forms: mechanochemical synthesis of an Indomethacin-Caffeine system. Cryst. Growth Des. 17 (11), 5744–5752.

Cabiscol, R., Shi, H., Wünsch, I., Magnanimo, V., Finke, J.H., Luding, S., Kwade, A., 2020. Effect of particle size on powder compaction and tablet strength using limestone. Adv. Powder Technol. 31 (3), 1280–1289.

Chen, J., Sarma, B., Evans, J.M.B., Myerson, A.S., 2011. Pharmaceutical crystallization. Cryst. Growth Des. 11 (4), 887–895.

Chierotti, M.R., Gobetto, R., 2008. Solid-state NMR studies of weak interactions in supramolecular systems. Chemical Communications. The Royal Society of Chemistry March 26, pp 1621–1634.

D'Addio, S.M., Prud'homme, R.K., 2011. Controlling Drug Nanoparticle Formation by Rapid Precipitation. Adv. Drug Deliv. Rev. 63 (6), 417–426.

Dong, Y., Ng, W.K., Hu, J., Shen, S., Tan, R.B.H., 2010. A continuous and highly effective static mixing process for antisolvent precipitation of nanoparticles of poorly water-soluble drugs. Int. J. Pharm. 386 (1–2), 256–261.

Dong, Y., Ng, W.K., Hu, J., Shen, S., Tan, R.B.H., 2014. Continuous production of redispersible and rapidly-dissolved fenofibrate nanoformulation by combination of microfluidics and spray drying. Powder Technol. 268, 424–428.

Eder, R.J.P., Radl, S., Schmitt, E., Innerhofer, S., Maier, M., Gruber-Woelfler, H., Khinast, J.G., 2010. Continuously seeded, continuously operated tubular crystallizer for the production of active pharmaceutical ingredients. Cryst. Growth Des. 10 (5), 2247–2257.

Eichie, F.E., Kudehinbu, A.O., 2009. Effect of particle size of granules on some mechanical properties of paracetamol tablets. African J. Biotechnol. 8 (21), 5913–5916.

Fell, J.T., Newton, J.M., 1970. Determination of Tablet strength by the diametral-compression test. J. Pharm. Sci. 59 (5), 688–691.

Geppi, M., Mollica, G., Borsacchi, S., Veracini, C.A., 2008. Solid-state NMR studies of pharmaceutical systems. Appl. Spectrosc. Rev. 43 (3), 202–302.

Hadiwinoto, G.D., Kwok, P.C.L., Tong, H.H.Y., Wong, S.N., Fung, S., Lakerveld, R., 2019. Integrated continuous plug-flow crystallization and spray drying of pharmaceuticals for dry powder inhalation.

Heider, P.L., Born, S.C., Basak, S., Benyahia, B., Lakerveld, R., Zhang, H., Hogan, R., Buchbinder, L., Wolfe, A., Mascia, S., et al., 2014. Development of a multi-step synthesis and workup sequence for an integrated, continuous manufacturing process of a pharmaceutical. Org. Process Res. Dev. 18 (3), 402–409.

Horn, D., Rieger, J., 2001. Organic nanoparticles in the aqueous phase—theory, experiment, and use. Angew. Chemie Int. Ed. 40 (23), 4330.

Hu, J., Ng, W.K., Dong, Y., Shen, S., Tan, R.B.H., 2011. Continuous and scalable process for water-redispersible nanoformulation of poorly aqueous soluble APIs by antisolvent precipitation and spray-drying. Int. J. Pharm. 404 (1–2), 198–204.

Jiang, M., Braatz, R.D., 2019. Designs of continuous-flow pharmaceutical crystallizers: developments and practice. CrystEngComm 3534–3551.

Jiang, M., Zhu, Z., Jimenez, E., Papageorgiou, C.D., Waetzig, J., Hardy, A., Langston, M., Braatz, R.D., 2014. Continuous-flow tubular crystallization in slugs spontaneously induced by hydrodynamics. Cryst. Growth Des. 14 (2), 851–860.

Keck, C., Muller, R., 2006. Drug nanocrystals of poorly soluble drugs produced by high pressure homogenisation. Eur. J. Pharm. Biopharm. 62 (1), 3–16.

Kumar, A., Davern, P., Hodnett, B.K., Hudson, S.P., 2019. Carrier particle mediated stabilization and isolation of valsartan nanoparticles. Colloids Surf. B Biointerfaces 175, 554–563.

Lakerveld, R., Benyahia, B., Braatz, R.D., Barton, P.I., 2013. Model-based design of a plant-wide control strategy for a continuous pharmaceutical plant. AIChE J. 59 (10), 3671–3685.

Lakerveld, R., Benyahia, B., Heider, P.L., Zhang, H., Wolfe, A., Testa, C.J., Ogden, S., Hersey, D.R., Mascia, S., Evans, J.M.B., et al., 2015. The application of an automated control strategy for an integrated continuous pharmaceutical pilot plant. Org. Process Res. Dev. 19 (9), 1088–1100.

Lu, X., Xu, W., Hanada, M., Jermain, S.V., Williams, R.O., Su, Y., 2019. Solid-state NMR analysis of crystalline and amorphous indomethacin: an experimental protocol for full resonance assignments. J. Pharm. Biomed. Anal. 165, 47–55.

Mascia, S., Heider, P.L., Zhang, H., Lakerveld, R., Benyahia, B., Barton, P.I., Braatz, R.D., Cooney, C.L., Evans, J.M.B., Jamison, T.F., et al., 2013. End-to-end continuous manufacturing of pharmaceuticals: integrated synthesis, purification, and final dosage formation. Angew. Chemie - Int. Ed. 52 (47), 12359–12363.

Matteucci, M.E., Hotze, M.A., Johnston, K.P., Williams, R.O., 2006. Drug nanoparticles by antisolvent precipitation: mixing energy versus surfactant stabilization. Langmuir 22 (21), 8951–8959.

Myerson, A.S., Krumme, M., Nasr, M., Thomas, H., Braatz, R.D. Control systems engineering in continuous pharmaceutical manufacturing May 20-21, 2014

Continuous Manufacturing Symposium. J. Pharm. Sci. John Wiley and Sons Inc. March 2015, pp 832–839.
Nagy, Z.K., Braatz, R.D., 2012. Advances and new directions in crystallization control. Annu. Rev. Chem. Biomol. Eng. 3 (1), 55–75.
Pandey, K., Chatte, A., Dalvi, S., 2018. Continuous production of aqueous suspensions of ultra-fine particles of curcumin using ultrasonically driven mixing device. Pharm. Dev. Technol. 23 (6), 608–619.
Paudel, A., Geppi, M., Van Den Mooter, G., 2014. Structural and dynamic properties of amorphous solid dispersions: the role of solid-state nuclear magnetic resonance spectroscopy and relaxometry. J. Pharm. Sciences. John Wiley and Sons Inc. September 1, pp 2635–2662.
Pitt, K.G., Heasley, M.G., 2013. Determination of the tensile strength of elongated tablets. Powder Technol. 238, 169–175.
Plumb, K., 2005. Continuous processing in the pharmaceutical industry: changing the mind set. Chem. Eng. Res. Des. 83 (6 A), 730–738.
Poechlauer, P., Manley, J., Broxterman, R., Gregertsen, B., Ridemark, M., 2012. Continuous processing in the manufacture of active pharmaceutical ingredients and finished dosage forms: an industry perspective. Org. Process Res. Dev. 16 (10), 1586–1590.
Quon, J.L., Zhang, H., Alvarez, A., Evans, J., Myerson, A.S., Trout, B.L., 2012. Continuous Crystallization of Aliskiren Hemifumarate.
Rogers, T.L., Gillespie, I.B., Hitt, J.E., Fransen, K.L., Crowl, C.A., Tucker, C.J., Kupperblatt, G.B., Becker, J.N., Wilson, D.L., Todd, C., et al., 2004. Development and characterization of a scalable controlled precipitation process to enhance the dissolution of poorly water-soluble drugs. Pharm. Res. 21 (11), 2048–2057.
Rossi, F., Cerreia Vioglio, P., Bordignon, S., Giorgio, V., Nervi, C., Priola, E., Gobetto, R., Yazawa, K., Chierotti, M.R., 2018. Unraveling the hydrogen bond network in a theophylline-pyridoxine salt cocrystal by a combined X-ray diffraction, solid-state NMR, and computational approach. Cryst. Growth Des. 18 (4), 2225–2233.
Schmidtke, R., Schröder, D., Menth, J., Staab, A., Braun, M., Wagner, K.G., 2017. Prediction of solid fraction from powder mixtures based on single component compression analysis. Int. J. Pharm. 523 (1), 366–375.
Skotnicki, M., Apperley, D.C., Aguilar, J.A., Milanowski, B., Pyda, M., Hodgkinson, P., 2016. Characterization of two distinct amorphous forms of valsartan by solid-state NMR. Mol. Pharm. 13 (1), 211–222.
Thorat, A.A., Dalvi, S.V., 2012. Liquid antisolvent precipitation and stabilization of nanoparticles of poorly water soluble drugs in aqueous suspensions: recent developments and future perspective. Chem. Eng. J. 181–182, 1–34.
Tierney, T., Bodnár, K., Rasmuson, Å., Hudson, S., 2017. Carrier particle design for stabilization and isolation of drug nanoparticles. Int. J. Pharm. 518 (1–2), 111–118.
Tierney, T.B., Guo, Y., Beloshapkin, S., Rasmuson, Å.C., Hudson, S.P., 2015. Investigation of the particle growth of fenofibrate following antisolvent precipitation and freeze−drying.
Tung, H.H., 2013. Industrial perspectives of pharmaceutical crystallization. Organic Process Research and Development. March 15, pp 445–454.
Veinberg, S.L., Johnston, K.E., Jaroszewicz, M.J., Kispal, B.M., Mireault, C.R., Kobayashi, T., Pruski, M., Schurko, R.W., 2016. Natural abundance 14N and 15N solid-state NMR of pharmaceuticals and their polymorphs. Phys. Chem. Chem. Phys. 18 (26), 17713–17730.
Virtanen, S., Antikainen, O., Räikkönen, H., Yliruusi, J., 2010. Granule size distribution of tablets. J. Pharm. Sci. 99 (4), 2061–2069.
Vogt, F.G., Roberts-Skilton, K., Kennedy-Gabb, S.A., 2013. A solid-state NMR study of amorphous ezetimibe dispersions in mesoporous silica. Pharm. Res. 30 (9), 2315–2331.
Wong, S.Y., Tatusko, A.P., Trout, B.L., Myerson, A.S., 2012. Development of continuous crystallization processes using a single-stage mixed-suspension, mixed-product removal crystallizer with recycle. Cryst. Growth Des. 12 (11), 5701–5707.
Zhang, H., Quon, J., Alvarez, A.J., Evans, J., Myerson, A.S., Trout, B., 2012. Development of continuous anti-solvent/cooling crystallization process using cascaded mixed suspension, mixed product removal crystallizers. Org. Process Res. Dev. 16 (5), 915–924.